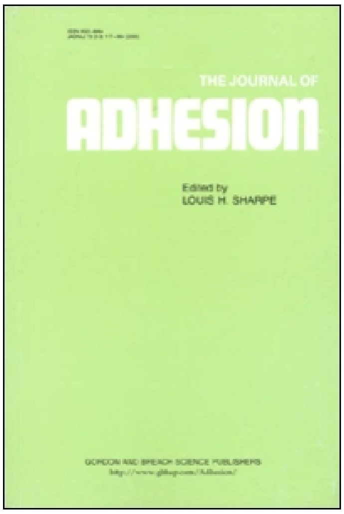

The Journal of Adhesion
Publication details, including instructions for authors and subscription information:
http://www.informaworld.com/smpp/title~content=t713453635

Relaxation Properties of Pressure-sensitive Adhesives upon Withdrawal of Bonding Pressure

Mikhail B. Novikov[a]; Tatiana A. Borodulina[a]; Sergey V. Kotomin[a]; Valery G. Kulichikhin[a]; Mikhail M. Feldstein[a]
[a] Russian Academy of Sciences, A. V. Topchiev Institute of Petrochemical Synthesis, Moscow, Russia

To cite this Article Novikov, Mikhail B. , Borodulina, Tatiana A. , Kotomin, Sergey V. , Kulichikhin, Valery G. and Feldstein, Mikhail M.(2005) 'Relaxation Properties of Pressure-sensitive Adhesives upon Withdrawal of Bonding Pressure', The Journal of Adhesion, 81: 1, 77 — 107

To link to this Article: DOI: 10.1080/00218460590904462

URL: http://dx.doi.org/10.1080/00218460590904462

The Journal of Adhesion, 81:77–107, 2005
Copyright © Taylor & Francis Inc.
ISSN: 0021-8464 print/1545-5823 online
DOI: 10.1080/00218460590904462

Taylor & Francis
Taylor & Francis Group

Relaxation Properties of Pressure-sensitive Adhesives upon Withdrawal of Bonding Pressure

Mikhail B. Novikov
Tatiana A. Borodulina
Sergey V. Kotomin
Valery G. Kulichikhin and Mikhail M. Feldstein
A. V. Topchiev Institute of Petrochemical Synthesis, Russian Academy of Sciences, Moscow, Russia

Relaxation properties of pressure-sensitive adhesives (PSA) have been studied with the squeeze-recoil tester used in the regime of parallel-plate dilatometer under conditions imitating the removal of compressive force in the course of adhesive bond formation. The relaxation properties of PSAs are compared with their adhesive behavior measured using the 180-Deg Peel Test. Two classes of PSAs are considered: 1) conventional rubbery adhesives based on the mixtures of styrene-isoprene-styrene (SIS) block copolymer with a tackifier resin and a plasticizer, and butyl rubber plasticized with low-molecular-weight polyisobutylene, and 2) hydrophilic PSAs composed of the blends of high-molecular-weight poly(N-vinyl pyrrolidone) (PVP) with oligomeric polyethylene glycol (PEG). By comparing the adhesive and relaxation behaviors of different PSAs, the relaxation criteria for pressure-sensitive adhesion have been stated. Relaxation behavior of the examined PSAs demonstrates two values of retardation time: the shorter retardation time of 10–70 sec and the longer time of 300–660 sec. These times can be associated, respectively, with small- and large-scale mechanisms of strain recovery. By comparing the relaxation and adhesive properties of PVP-PEG blend (which involves the formation of a hydrogen-bonded network through both terminal hydroxyl groups in PEG short chains) with the properties of covalently crosslinked copolymers of vinyl pyrrolidone (VP) with PEG-diacrylate and comb-like VP copolymers with PEG-monomethacrylate, the contributions of covalent crosslinking and H-bonding network have been characterized.

Received 25 June 2004; in final form 26 October 2004.

This research was sponsored in part by Corium International, Inc., USA, under grant RC0-1357 of the U.S. Civilian Research & Development Foundation. We thank Academician Nicolai A. Platé, Prof. Costantino Creton, Prof. Anatoly E. Chalykh, Dr. Gary W. Cleary, and Dr. Parminder Singh for stimulating discussion. Special thanks to Dr. Ivan L. Valuev for the synthesis of crosslinked copolymers.

Address correspondence to Dr. Mikhail M. Feldstein, A. V. Topchiev Institute of Petrochemical Synthesis, Russian Academy of Sciences, 29, Leninsky prosp., 119991, Moscow, Russia. E-mail: mfeld@ips.ac.ru

Keywords: Retardation times; Pressure-sensitive adhesion in hydrophilic and rubbery adhesives; Poly(N-vinyl pyrrolidone)-poly(ethylene glycol) adhesive blends; Contribution of hydrogen bonding; Butyl rubber; Styrene-isoprene-styrene block copolymer

INTRODUCTION

Pressure-sensitive adhesion can be treated as a three-stage continuous process that proceeds with time in response to the application of mechanical stress. The first stage takes place when a compressive force is applied to the adhesive film, providing the formation of an adhesive bond. The second stage occurs when the bonding force is withdrawn and the adhesive relaxes, releasing part of the energy expended in the course of the first stage. The third stage is a process of adhesive bond failure under applied debonding stress. Adhesive and mechanical (rheological) properties of viscoelastic polymer materials are time dependent [1]. These properties come into play when the material is subjected to flow under a compressive force in the course of adhesive bond formation, or deformed under a detaching force. Both these stages require an input of energy. Under applied force, part of the energy imparted is irrecoverably dissipated through a mechanism of viscous flow, while another part is stored and can be released elastically upon the removal of the bonding or detaching force. The dissipation never takes place instantaneously. As a result, the response of the adhesive material lags behind the application of the deformation force. For this reason, adhesive properties are time dependent and this dependence cannot be ignored when dealing with such materials. Although the mechanical properties of pressure-sensitive adhesives (PSAs) are the subject of extensive study and reviewed in relevant books [2, 3], nevertheless the significance of relaxation properties for pressure-sensitive adhesion remains inadequately understood [4].

Time-dependent mechanical properties are traditionally characterized in terms of so-called response times, and in fact are almost always characterized by a distribution of such times [1]. If a material is strained, a stress relaxes and the response times are relaxation times. If a strain is retarded under applied stress, the response times are retardation times. The relaxation and retardation times are not identical. When ranking both sets in ascending or descending order, they alternate, that is, the retardation times are intercalated between the relaxation times [5].

Each response time is associated with relevant spectral strength that may be a modulus, G_i, or a compliance, J_i. The time dependence of a material is thus revealed in a finite, discrete set of response times and their associated spectral strengths. When a stress is removed and a strain recovery occurs, this set is $\{J_i, \tau_i\}$ [6, 7]:

$$J = J_0 + \sum_{i=1}^{i=n} J_i(1 - e^{-t/\tau_i}) \tag{1}$$

where J_i is the compliance (Pa^{-1}) in the i-element of a structure and τ is the retardation time (s). As $\mathrm{t} \to \infty,\ J_0 \to 0$. The corresponding value of relaxation modulus can be evaluated with Equation (1) as the reciprocal of the compliance, $G_i = 1/J_i$.

The mechanism of pressure-sensitive adhesion requires coupling of two mutually inconsistent and apparently conflicting properties. In the process of adhesive bond formation, a PSA material should behave like a viscous liquid, which flows under a slight compressive force and coats the surface of a substrate. The mode of deformation, providing the adhesive bond formation, is typically in shear [8]. At the stage of adhesive bond failure, the same PSA material should deform like a soft, rubber-like solid that can store elastic energy. Taking into account dramatic distinctions between the deformation mechanisms of the PSA polymers in the processes of adhesive bonding and debonding, we believe that the relaxation properties of adhesives can also be different in various stages of adhesive bonding and debonding. In this article we consider the retardation times of PSAs upon the removal of the compressive force in the final stage of adhesive bond formation. The relaxation properties under the compressive bonding force and in the course of debonding will be a subject of our future publications.

A common method of PSA testing is the measuring of peel adhesion [1]. For high angle peel, where the shear mechanism is negligible and extension dominates, the peel force, P, relates to the viscoelastic characteristics of the adhesive material by the well-known Kaelble equation [9]. For 180-deg peeling with a fixed peel rate, the Kaelble equation reads as follows:

$$P = \frac{b \cdot l \cdot \sigma_f^2}{4E} \tag{2}$$

where E is tensile modulus, σ_f is a critical value of ultimate tensile stress at a fracture of the PSA material under uniaxial drawing, b is the width, and l is the thickness of adhesive layer. Equation (2) can easily be modified to express the peel adhesion, P, as an explicit function of the relaxation time, τ, and self-diffusion coefficient, D, of a PSA polymer [10, 11]. Indeed, let us assume in the first approximation that an adhesive can be characterized with a single apparent relaxation time, τ, and a microviscosity (or monomer-monomer friction coefficient of the polymer chain), η. Taking into account that according to the Maxwell model of linear viscoelasticity, $E = 3\eta/\tau$ [7], we can further express the microviscosity through the self-diffusion coefficient of the polymer segment, D, using the De Gennes Equation [12]:

$$D = \frac{kT}{\eta \cdot a \cdot N}$$

where N is a number of monomer units of size a in the polymer chain segment. Substitution of the obtained values into the Kaelble Equation (2) yields

$$P = b \cdot l \cdot \frac{a \cdot N_A \cdot D \cdot \tau}{12RT} \cdot \sigma_f^2 \tag{3}$$

where a is the size of the polymer chain segment, N_A is Avogadro's number, R is the universal gas constant, and T is temperature.

Equation (3) is illustrative but holds only in the linear elastic region of the deformation process and ignores the existence of the spectrum of relaxation times and, thus, provides a very crude tool, which is applicable only for qualitative estimations. Nevertheless, it predicts illustratively the significance of diffusion and relaxation processes for the adhesive behavior of polymers. It is worthy of note that Equation (3) has been derived on the basis of the analysis of the deformation contribution to peel adhesion without resorting to a so-called diffusion theory of adhesion. According to Equation (3), the pressure-sensitive adhesion requires a coupling of high molecular mobility, embedded by the self-diffusion coefficient of adhesive polymer segment, D, with long-term relaxation processes outlined by large values of the relaxation times, τ, and a high cohesive strength of the adhesive polymer, expressed in terms of the ultimate tensile stress at the break of the stretched adhesive, σ_f [11].

The present work is intended to be an important part of our investigations aimed at elucidating the molecular origins of pressure-sensitive adhesion [10, 11, 13, 14] and the development of a new class of hydrophilic PSAs based on the miscible blends of nonadhesive parent polymers [15–17]. Those involve a hydrogen or electrostatic bonding between the components of the adhesive polymer blends [18–21], which results in the occurrence of pressure-sensitive adhesion. A stoichiometric H-bonded complex formed under mixing of high-molecular-weight poly(N-vinyl pyrrolidone) (PVP) with short-chain poly(ethylene glycol) (PEG), which is responsible for the adhesion in PVP-PEG blends, serves as a convenient model to gain a molecular insight into the nature of pressure-sensitive adhesion.

Adhesive behavior of PVP-PEG blends as a function of composition and the amount of absorbed water has been evaluated using the Peel [22] and Probe Tack tests [23]. Although neither PVP nor PEG *per se* demonstrates any pressure-sensitive adhesion, their blends exhibit adhesion, and absorbed water can significantly influence the adhesive behavior of the PVP-PEG hydrogels. In fact, only the blends in a very narrow range of PEG content (in the vicinity of 36 wt.%) and amount of absorbed water (6–12%) provide high adhesion, whereas both PEG-underloaded and -overloaded blends as well as dry and over-moistened compositions reveal no or insignificant adhesion. It is precisely such behavior that makes the PVP-PEG system a very convenient model from which to elicit the molecular structure responsible for pressure-sensitive adhesion. For this purpose, we have to merely compare the structure and properties of adhesive and nonadhesive PVP-PEG blends.

The PVP-PEG interaction mechanism and the structure of the stoichiometric complex have been established with Fourier transformed infrared (FTIR) spectroscopy and differential scanning calorimetry (DSC) [18–21]. The PVP has been found to be soluble in liquid, low-molecular-weight fractions of PEG (200–600 g/mol), and immiscible with PEG of higher molecular weight [24, 25]. This behavior indicates that terminal hydroxyl groups of short-chain PEG are of crucial importance for PVP-PEG miscibility. Actually, according to FTIR data, the PVP-PEG miscibility is due to hydrogen bonding of both terminal proton-donating OH groups of the PEG to the complementary proton-accepting carbonyl groups in the repeat units of the PVP backbone [18, 19]. Because every PEG macromolecule bears two reactive groups at opposite chain ends, the PEG is able to noncovalently crosslink the longer PVP macromolecules. Formation of a hydrogen-bonded network in PVP-PEG blends leads to the enhanced cohesive strength and rubber-like behavior, established by means of dynamic mechanical analysis and a tensile test [26]. Location of reactive OH groups at the ends of comparatively long and flexible PEG chains causes the formation of large free volume, measured as a function of PVP-PEG composition and amount of absorbed water with positron annihilation techniques [27]. It is large free volume that governs a liquid-like fluidity of the PVP-PEG blends. Large free volume provides also a high molecular mobility of PVP-PEG blends, examined using pulsed-field gradient nuclear magnetic resonance (PFG NMR) technique and evaluated in terms of self-diffusion [28, 29] and interdiffusion coefficients [24, 25].

Both the chemical composition and the structure of the PVP-PEG complex have nothing to do with those of conventional PSAs, which are mainly formulated on the basis of hydrophobic rubbers. Nevertheless, we believe that common properties found for the PVP-PEG complex and for conventional adhesives might be of particular importance for their adhesive behavior. Consequently, in order to elucidate general criteria for pressure-sensitive adhesion we need to compare the properties of those PVP-PEG blends, which provide best adhesion, with the properties of conventional PSAs, and find similarities. Such an approach has been previously employed [26] to gain insight into the mechanical properties underlying pressure-sensitive adhesion. In this paper we employ this approach to establish the relaxation criteria for pressure-sensitive adhesion.

If common features in the behavior of PVP-PEG and conventional PSAs are of particular importance for comprehending of the necessary conditions for pressure-sensitive adhesion, any distinctions might be due to the contribution of the network of hydrogen bonds, which is only typical for PVP-PEG adhesive hydrogels. Based on a comparison of the behavior of the PVP-PEG adhesive with that of conventional hydrophobic PSAs, we have come to the following conclusions:

1) The major determinant of the pressure-sensitive adhesion at a molecular level is a specific value of the ratio of high cohesive interaction energy to large free volume in adhesive polymers [13, 22].
2) The physical significance of the well-known Dahlquist's criterion for tack [30] at a molecular level is that it characterizes the ratio of the energy of cohesion to the free volume in terms of the elastic modulus [26]. For PSAs this modulus must be of the order of $1 - 5 \cdot 10^5$ Pa at large elongations, which are typical for adhesive bond failure.
3) A simple tensile test allows us an indirect and separate evaluation of the values of the cohesive interaction energy and the free volume through related values of ultimate tensile stress and maximum elongation at break, respectively [26].

In the following sections, we consider the relaxation properties of PVP-PEG blends of different composition, which provide different adhesion upon the removal of bonding pressure. The retardation spectra of hydrophilic PVP-PEG adhesives are compared with those for two types of hydrophobic PSAs:

1) a styrene-isoprene-styrene (SIS) block copolymer mixed with a plasticizer (low-molecular-weight isoprene rubber, Isolene, I) and a tackifier resin (Regalite, R), and
2) a blend of high-molecular-weight butyl rubber (BR) and a low-molecular-weight polyisobutylene (PIB)

MATERIALS AND METHODS

PVP ($M_w = 1{,}000{,}000$ g/mol) and PEG ($M_w = 400$ g/mol) were obtained from BASF (Ludwigshafen, Germany) as Kollidon K-90 and Lutrol E-400, respectively. Both polymers were used as obtained.

Adhesive films 250–300 μm in thickness were prepared by dissolving the PVP and PEG in a common solvent (ethyl alcohol) followed by casting the solution on a poly(ethylene terephthalate) (PET) backing film 60 μm in thickness and drying for 3 days at ambient temperature (20–22°C). The films were then dried for 2 hrs under vacuum, at 65°C. The adhesives were saturated with water by equilibrating in dessicators with controlled pressure of water vapor at ambient temperature for 6–7 days. The equilibrium content of sorbed water in PVP-PEG adhesive films ranged from 5 to 30%. Unsupported adhesive films 700 μm in thickness were produced by casting the solution onto PET release liner (0.6 mm in thickness) and drying for 3 days at ambient temperature. The uniform thickness of the PVP-PEG films was provided using the BYK-Gardner (Silver Spring, MD, USA) film casting knife. After blend-drying, the release liner was removed and unsupported PVP-PEG films were used in tensile test experiments.

Styrene-isoprene-styrene (SIS) block copolymer (Vector 4111) was obtained from Dexco Polymers (Houston, TX, USA). Tackifying resin, Regalite R 9100, was purchased from Hercules (Wilmington, DE, USA). The plasticizer Isolene 400 was obtained from Elementis Performance Polymers (Belleville, NJ, USA). Butyl Rubber 065 and PIB Vistanex LM-MH were supplied by Exxon Chemicals (Houston, TX, USA). Hydrophobic PSA DURO-TAK 34–4230 was purchased from National Starch & Chem. Corp. (Bridgewater, NJ, USA). All the materials were used as received. Polymer samples of hydrophobic PSA were prepared by direct mixing of components in a Haake mixer under 130°C (Thermo Haake, Karlsruhe, Germany). The compositions of hydrophobic adhesives are listed in Table 1. To produce adhesive

TABLE 1 Compositions of Hydrophobic Polymers Examined

Sample	Composition
SIS + I	SIS Vector 4111 (57% wt.)/Isolene 400 (43% wt.)
SIS + R	SIS Vector 4111 (50% wt.)/Regalite R9110 (50% wt.)
SIS + R + I	SIS Vector 4111 (36.4% wt.)/Regalite R9110 (27.2% wt.)/Isolene 400 (36.4% wt.)
B + PIB	BR 065 (60% wt.)/PIB Vistanex LM-MH (40% wt.)

films, prepared blends were compressed under a pressure of 0.5 MPa at 80°C until uniform films of 0.4 mm in thickness were obtained. Adhesive blends of DURO-TAK 34-4230 were obtained using the same procedure.

The copolymers of polyvinyl pyrrolidone (PVP) with poly(ethylene glycol-400) diacrylate (PVP-PEGDA), and monomethacrylate (PVP-PEGMMA) were prepared by radical copolymerization in water using a redox system (ammonium persulfate—N, N, N′ N′,-tetramethylethyl enediamine) as an initiator.

To evaluate relaxation properties of adhesives under the conditions modeling adhesive bond formation, a squeeze-recoil technique was employed, described in [28, 31] and shown schematically in Figure 1. The viscoelastic properties of the adhesives under a squeezing flow were measured on a parallel plate high-precision dilatometer based on DTMD thermomechanical analyzer, designed by Bureau of Unique Equipment of the Russian Academy of Sciences. A hydrogel sample of 0.5–1.5 mm in thickness has initially the same size as an upper cylindrical quartz rod of 6 mm in diameter with a flat end. In the course of the test, the sample is compressed between a bottom immovable plate and the upper cylindrical rod. At the beginning of the test, a fixed total force, *F*, is applied to the upper rod by means of weights 1–500 g, and the rod displacement [gap between the plates, *h(t)*] is measured with an accuracy of 1 μm as a function of time. As the compression proceeds, material is squeezed from a gap between the upper and the bottom plates, and the total compression area remains constant and equal to the cross section of the upper rod. Upon the removal of squeezing

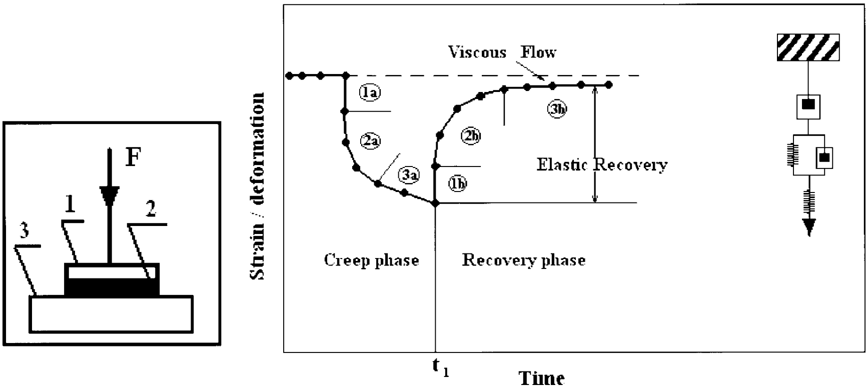

FIGURE 1 Schematic of the experimental setup for a squeeze-recoil test and typical view of the squeeze-recoil profile according to the Burgers model [7]. 1, upper plate; 2, polymer sample; 3, bottom plate.

force, the creep recovery occurs and the elastic sample returns more or less to its initial shape, lifting the upper rod. This stage of strain relaxation is termed "squeeze recoil." The retardation times and characteristic moduli of tested adhesives were estimated by nonlinear fitting of the experimental curves shown in Figure 2 with Equation (1) using Microsoft Origin 6.0 software and selecting a function of exponential association, which represents Equation (1), from the list of options offered by the computer program. For slow relaxation processes, the total time of measuring of sample thickness, h, was limited to 6000–7000 sec. Under the experimental conditions employed in this work (temperature of 18–22°C, relative humidity of surrounding atmosphere of 50–60%), over this observation time, the change in the amount of water absorbed by the sample was less than 1%. This total observation time corresponds to an average time of elastic recovery upon the withdrawal of compressive force of 2000 sec.

The adhesive joint strength of PVP-PEG hydrogels was evaluated by 180-Deg Peel testing as is earlier described [22] using an Instron 1221 Tensile Strength Tester (Instron, Canton, MA, USA) at different peeling rates. A low-density polyethylene (PE) film of 100 μm in

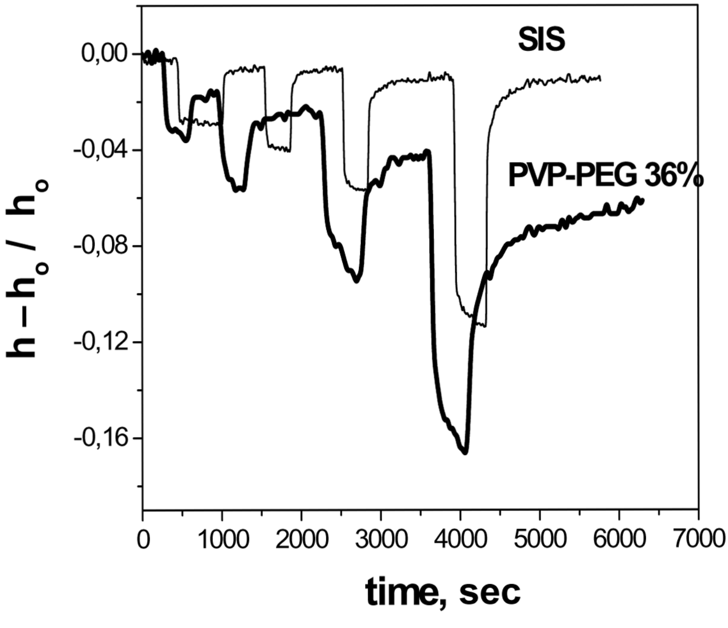

FIGURE 2 Squeeze-recoil profiles for SIS and PVP blend with 36% of PEG under stepwise increasing compressive force of 0.5, 1, 2, and 5 N.

thickness and 80 μm poly(ethylene terephthalate) (PET) film were employed as standard substrates. The time to attain a maximum strength of adhesive contact with the substrate was 20 min. This dwell time on the PE substrate prior to peeling has been found to be sufficient in order to provide the maximum strength of adhesive bond for all the PVP-PEG blends examined in this work [22].

RESULTS AND DISCUSSION

Squeeze-Recoil Behaviors of Pressure-Sensitive Adhesives

The very name pressure-sensitive adhesives implies the importance of their rheological behavior under a compressive force for their adhesive performance. A squeeze-recoil technique provides a close, informative, and illustrative model of all three stages of the process of adhesive bonding and debonding [32], namely an adhesive bond formation under compressive stress, relaxation of adhesive material upon the removal of the bonding stress, and the failure of adhesive joint under applied debonding stress. Although this technique is simple to use, it really provides true material parameters for Newtonian and Power Law fluids [33, 34]. However, this relates only to the stage of squeezing flow under compressive force, whereas in this work we consider the behavior of adhesive materials at the stage of elastic recovery as the squeezing force is removed. For this purpose, we use the squeeze-recoil tester as a high precision parallel-plate dilatometer to measure the retardation of adhesive material. Elastic recovery is a standard method for determination of retardation properties of solid polymers and viscoelastic materials [35]. The recovery process is, in fact, only applicable to the material that fills the gap between the parallel plates of the squeeze-recoil tester. The part of the material that has been irreversibly squeezed out does not play a role in the recovery process, because it relaxed upon leaving the gap.

Typical squeeze-flow displacement-time curves for SIS triblock copolymer and PVP-PEG adhesive blend are shown in Figure 2. A remarkable agreement is observed between the squeeze-recoil behaviors of real materials and the ideal Burgers model of viscoelastic body [7] illustrated in Figure 1.

The Burgers model of viscoelasticity can be applied to describe the squeeze-recoil curves of PSAs. The Burgers model represents the combination of springs and dashpots outlined by the Kelvin–Voigt model of a viscoelastic solid and the Maxwell model of a viscoelastic liquid, which are linked to each other in series [7]. Figure 1 shows the squeeze-recoil profile of the idealized viscoelastic material according to the Burgers model. When the material is subjected to compressive stress, three different strain responses can be observed [7]:

1a) step of instantaneous elastic response because of the Maxwell spring;
2a) gradual strain development related to the Kelvin–Voigt element, which reaches its equilibrium value with time tending to infinity; and
3a) purely viscous response of the Burgers model related to the Maxwell dashpot that occurs as the Kelvin–Voigt element has attained its equilibrium. The slope of the strain-time curve is then constant and is equal to the shear rate.

When the compressive stress is removed, the Burgers model recovers in a two-step manner:

1b) strain reduces instantaneously by the elastic response, and
2b–3b) strain reaches a value that is equal to permanent, nonrecoverable strain and represents the viscous flow of the Maxwell dashpot.

The agreement between the behaviors of idealized Burgers model (Figure 1) and real adhesives shown in Figure 2 is qualitative evidence that the examined adhesives behave like linear viscoelastic systems, implying the applicability of the squeeze-recoil test for characterization of the relaxation properties of the adhesives upon the removal of compressive force.

As a fixed compressive force is applied to a sample, the gap (h) between the upper and bottom plates of a tester, which is equal to the sample thickness, decreases gradually (Figure 2). The higher the squeezing stress, the more the SIS rubber and PVP-PEG hydrogel are deformed. Under comparable compressive force, the PVP-PEG adhesive is compressed to a greater extent than the SIS rubber, indicating that the PVP-PEG hydrogel is softer.

The deformation of the samples under squeeze flow is partly recoverable. As the compressive force is removed, the sample tends to returns to its initial shape. The profile of the squeeze recoil is indicative of the elastic contribution and relaxation properties of the material. As is evident from the curves shown in Figure 2, the SIS rubber recovers its initial thickness better as compared with the PVP-PEG adhesive hydrogel. For the latter, the viscous dissipation of mechanical energy is much more pronounced.

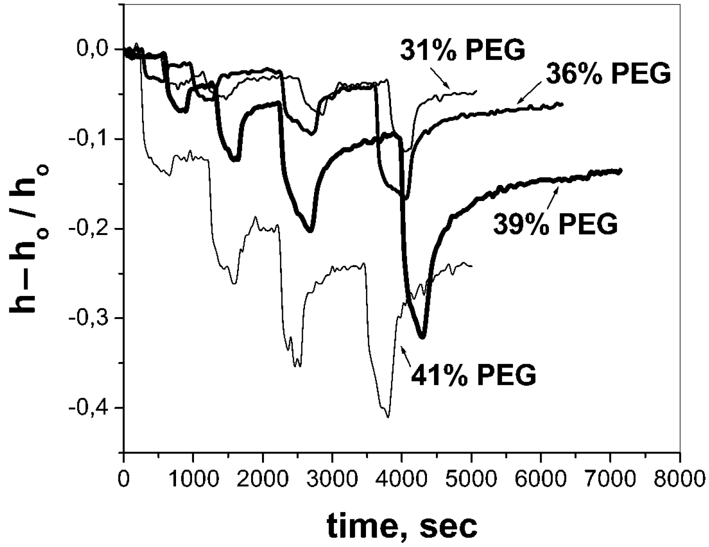

FIGURE 3 Effect of PEG content on squeeze-recoil profiles of PVP-PEG blends under stepwise increasing compressive force of 0.5, 1, 2, and 5 N.

Figure 3 illustrates the effect of PEG concentration on the squeeze-recoil profiles of PVP-PEG blends under stepwise increasing compressive force. The higher the PEG content, the greater the contribution of plastic deformation. Longer time is then required to recover the equilibrium thickness of the hydrogel upon removal of compressive stress, indicating that the relaxation time grows with the rise in PEG concentration.

Retardation Times Featured for Hydrophilic PVP-PEG Adhesives

For evaluation of the relaxation properties of adhesives from the data shown in Figures 2 and 3, the values of relative displacement at a recovery step, $(h - h_0)/h_0$, have been taken with a positive sign and plotted against time in Figures 4 and 5. Division of the $(h - h_0)/h_0$ value by the removed stress yields the compliance, J. The points represent the measured values, whereas the lines are the results of the data fitting with Equation (1). As follows from Figures 4 and 5 and the data in Table 2, Equation (1) provides a fairly reasonable fit with a regression coefficient that is always no less than 0.98. Adequate fitting is obtained taking into account two terms in Equation (1),

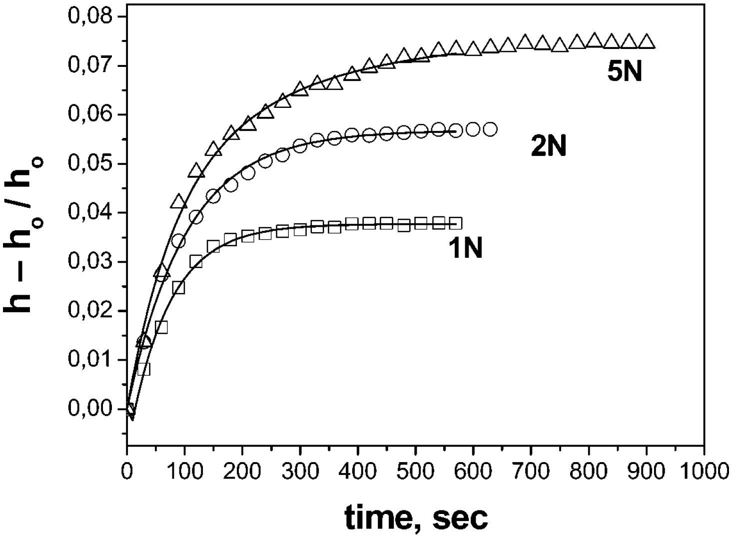

FIGURE 4 Impact of compressive force on the kinetics of strain recovery upon the removal of compressive force for PVP-PEG (36 wt.%) adhesive.

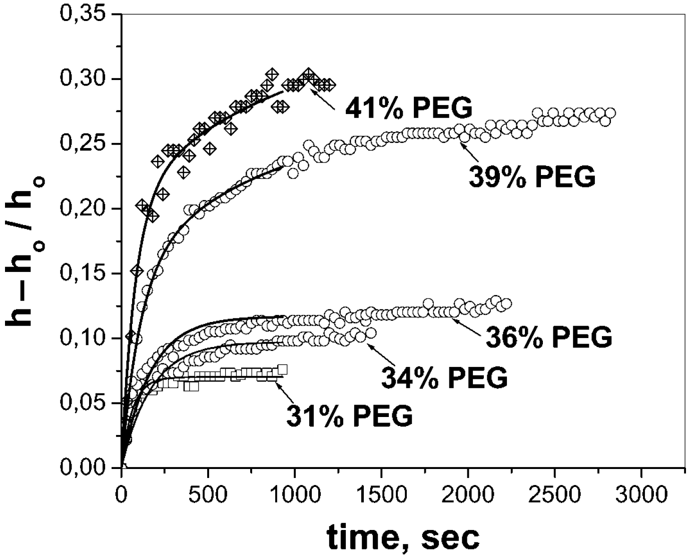

FIGURE 5 Effect of PEG concentration on the kinetics of strain recovery for PVP-PEG blends.

TABLE 2 Effect of Compressive Force on the Relaxation Behavior of PVP Blends Containing Different Amounts of PEG-400 and 8–9% of Absorbed Water and SIS-Based the DURO-TAK 34–4230 PSA

PEG content, wt.%	Compressive force, N	J, Pa^{-1}	G, MPa	τ, s	R^2	J_1, Pa^{-1}	G$_1$, MPa	τ_1, s	J_2, Pa^{-1}	G$_2$, MPa	τ_2, s	R^2
31%	1	7.8E-7 ± 4.15E-10	1.27	147 ± 3	0.97	2.03E-7 ± 3.9E-8	4.9	43 ± 6	2.94E-7 ± 3.8E-8	3.4	149 ± 13	0.99
	2	5.17E-7 ± 8.7E-9	1.97	89 ± 9	0.96	2.07E-7 ± 1.8E-8	4.8	33 ± 10	3.4E-7 ± 1.72E-8	3.0	156 ± 7	0.99
	5	3.97E-7 ± 4.2E-9	2.52	63 ± 5	0.97	2.9E-7 ± 2.7E-8	3.46	32 ± 7	1.3E-7 ± 2.1E-8	7.69	298 ± 40	0.99
34%	1	8E-7 ± 4E-9	1.30	33 ± 2	0.97	5.4E-7 ± 3.7E-8	1.85	48 ± 2.8	2.86E-7 ± 3.6E-8	3.5	185 ± 19	0.99
	2	7.95E-7 ± 3.84E-9	1.59	44 ± 7	0.96	3.97E-7 ± 4.2E-9	2.52	13 ± 0.3	2.68E-7 ± 3.99E-9	3.73	127 ± 2.3	0.99
	5	5.4E-7 ± 4.2E-9	1.82	172 ± 12	0.96	3.18E-7 ± 2.6E-8	3.23	59 ± 6	3E-7 ± 1.6E-8	3.45	619 ± 35	0.99
36%	1	9.75E-7 ± 1.13E-8	1.03	70 ± 5	0.96	7.7E-7 ± 1.75E-8	1.3	46 ± 2	3.03E-7 ± 9.37E-9	3.3	429 ± 51	0.99
	2	7.4E-7 ± 1.3E-8	1.35	77 ± 8	0.97	4.6E-7 ± 6.4E-8	2.17	26 ± 8	3.5E-7 ± 4.4E-8	2.94	325 ± 100	0.99
	5	6.6E-7 ± 5E-8	1.52	167 ± 9	0.96	4.45E-7 ± 1.82E-8	2.27	68 ± 5.5	2.6E-7 ± 1.3E-8	3.77	742 ± 96	0.99
39%	1	2.47E-6 ± 6.3E-9	0.41	42 ± 0.8	0.96	2.01E-6 ± 2.8E-7	0.5	63 ± 1.4	1.13E-6 ± 1.2E-7	0.88	444 ± 34	0.99
	2	2.47E-6 ± 4.08E-8	0.40	58 ± 7.4	0.97	1.74E-6 ± 2.4E-8	0.57	18 ± 4	1.09E-6 ± 1.76E-8	0.9	371 ± 23	0.99
	5	1.6E-6 ± 1.9E-8	0.63	143 ± 9.3	0.97	1.16E-6 ± 1.6E-7	0.86	80 ± 14	7.5E-7 ± 2E-7	1.32	940 ± 158	0.99
41%	1	2.11E-6 ± 2.65E-8	0.47	52 ± 4	0.96	1.72E-6 ± 2.7E-8	0.58	30 ± 0.8	7.79E-7 ± 2.6E-8	1,3	394 ± 60	0.99
	2	1.58E-6 ± 1.91E-8	0.63	169 ± 10	0.97	7.75E-7 ± 7.19E-8	1.29	47 ± 7	9.6E-7 ± 5.1E-8	1.04	450 ± 64	0.99
	5	1.45E-6 ± 9E-9	0.69	282 ± 10	0.97	8.51E-7 ± 3.13E-8	1.18	107 ± 6	7E-7 ± 2.5E-8	1.44	856 ± 60	0.99
SIS-based DURO-TAK PSA	0.5	2.68E-6 ± 9E-9	0.37	39 ± 1	0.96		—	—		—	—	—
	1	4.02E-6 ± 3.2E-8	0.25	31.7 ± 3	0.96	3.3E-6 ± 1.08E-7	0.74	17 ± 2	8.9E-7 ± 8.7E-8	2.48	356 ± 90	0.99
	5	1.69E-6 ± 1.1E-8	0.59	28.8 ± 3	0.97	1.35E-6 ± 2.38E-8	0.3	17 ± 1.7	4.02E-7 ± 2.13E-8	1.12	400 ± 40	0.99

whereas adding third and fourth terms does not improve the fit, and gives corresponding retardation times, which fall within the range of deviations from the value of a longer retardation time found with Equation (1) in two-term form. Using Equation (1) with a single retardation time does not provide adequate fitting (relevant regression coefficients lie normally around 0.96; see Table 2). In this work subscripts 1 and 2 correspond, respectively, to the shorter and longer retardation times, whereas the lack of the subscript implies that the fitting is provided with Equation (1) including only a single term.

The coefficients of regression with Equation (1) for the squeeze-recoil profiles shown in Figures 4 and 5 are listed in Table 2 along with relevant values of evaluated retardation times and compliances. They are also presented in Figures 6 and 7 as functions of PEG content in adhesive blends with PVP. Two reliably different retardation times are found for the PVP-PEG adhesives, which in their magnitudes are about one decade apart: the shorter time, τ_1 (in the range of 10–110 s) and the longer one ($\tau_2 \approx 120-950\,\text{s}$). Within the framework of the Burgers model of viscoelasticity, the shorter retardation or relaxation time is mainly associated with the elastic contribution of the spring element to strain recovery, whereas the longer time

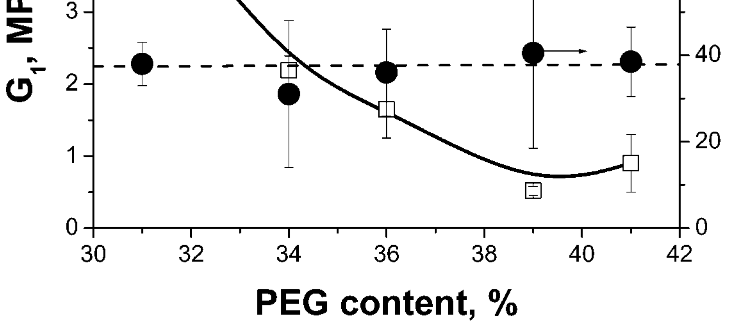

FIGURE 6 Shorter retardation time and corresponding modulus as a function of the concentration of plasticizer (PEG) in PVP-PEG adhesive blends. The data are averaged for two values of compressive force (1 and 2 N).

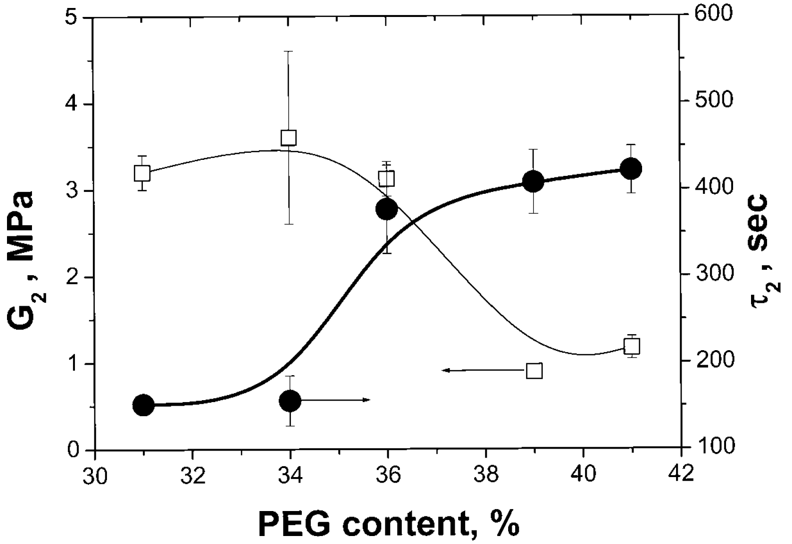

FIGURE 7 Longer retardation time and corresponding modulus plotted versus PEG concentration in PVP-PEG adhesive blends. The data are averaged for two values of compressive force (1 and 2 N).

characterizes the behavior of coupled dashpot and spring elements of the model and the rate of strain recovery under dissipation of applied energy. The mechanism of the latter process involves large-scale rearrangement of the structure of the polymer material *via* translational movement (diffusion) of polymer segments and entire macromolecules. This process normally takes a much longer time than the elastic recovery of polymer chain conformations. The longer process may be also associated with entanglements of polymer chains. The shorter retardation time relates mainly to the restoration of the original conformation of polymer segments.

As is seen from Figures 6 and 7, with increasing PEG concentration in the blends, the shorter retardation time has been found to be nearly constant, whereas the longer time increases gradually. The relevant values of corresponding moduli gradually reduce with PEG content. The increase in longer retardation time under PEG addition is also easily observable in Figure 3 on the slowing down of strain recovery upon the removal of compressive force.

As is obvious from the data listed in Table 2, under relatively moderate values of compressive force the values of retardation times and corresponding moduli are practically independent of applied compressive stress. However, at comparatively high shear stress (compressive force of 5 N and higher) both the retardation times and corresponding moduli tend to increase. Actually, the higher the stress, the larger the molecular rearrangements occurring in strained material, and the longer the time required for relaxation. The values of retardation times and moduli at relatively moderate compressive forces of 1 and 2 N can be considered as material characteristics. As a rule, in order to demonstrate the effects of composition on the spectra of retardation times in the examined PSAs, we use the values of retardation time and associated modulus averaged for compressive force of 1 and 2 N.

The retardation times and corresponding moduli are not independent material characteristics but are codependent quantities. As follows from the data in Table 2 and Figure 8, in the course of PVP plasticization with PEG, the higher values of longer retardation time are usually associated with lower values of corresponding modulus. The behavior of the shorter retardation times and moduli disobeys this law because of the strong impact of PEG content on G_1 modulus, while the shorter retardation time is invariable with the composition of PVP-PEG blends (Figure 6). The inverse proportion between the retardation time and corresponding modulus, which is the case for all the polymer blends studied in this work, implies the applicability of the Maxwell, Kelvin–Voight, and Burgers models of viscoelasticity

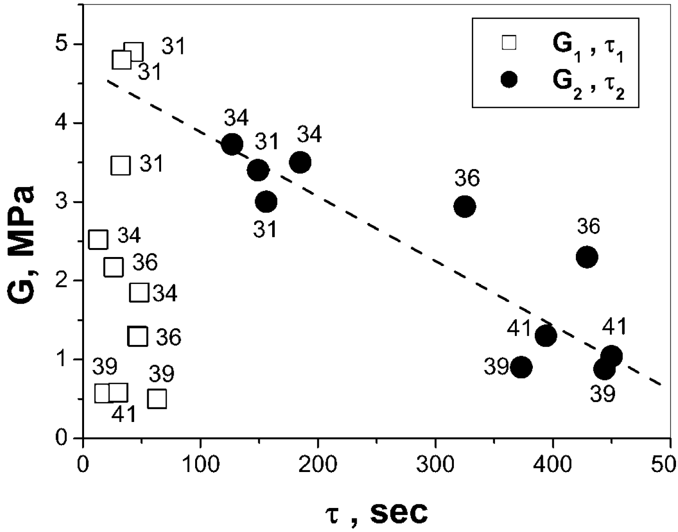

FIGURE 8 Relationship between retardation times and corresponding moduli for PVP-PEG blends. The PEG contents (wt.%) are indicated.

($G = \eta/\tau$) for description of behavior of the hydrophilic PVP-PEG and hydrophobic adhesives. While the comparison of idealized behavior of the Burgers model illustrated in Figure 1 with the squeeze-recovery profiles of real adhesives (Figure 2) qualitatively characterizes these adhesives as linear viscoelastic systems, the data in Figure 8 provide quantitative support in favor of this observation and imply that the values of retardation times and corresponding moduli evaluated in this work can be treated as true material constants.

Retardation Times in Hydrophobic Pressure-Sensitive Adhesives

Many hydrophobic elastomers have been used to produce PSAs, but generally the elastomers have to be blended with tackifiers and plasticizers in order to obtain the proper adhesion. In a PSA formulation, the rubbery polymer provides the elastic component, while a low-molecular-weight tackifying resin and a plasticizer constitute the viscous components. Most parent elastomers *per se* do not have the proper rheology to be PSAs. Typically, the addition of tackifier raises the glass transition temperature, T_g, lowers the plateau modulus by diluting the chain entanglements of the elastomer and increases the ratio of viscous to elastic response of the elastomer/tackifier blend, improving both the bond-making and bond-breaking process. Plasticizers demonstrate a similar effect on rheology, but cause T_g reduction. It is, therefore, of particular interest to trace how the formulation process affects the relaxation properties of a composite PSA.

In this work we use a styrene-isoprene-styrene (SIS) block copolymer and butyl rubber (BR) as PSA-giving elastomers. Hydrocarbon resin (Regalite R9100, R) has been employed as a tackifier. The Regalite is a partially hydrogenated resin with a specific balance of aliphatic and aromatic groups. As an SIS plasticizer, a low-molecular-weight polyisoprene rubber (Isolene, I) has been used. The pressure-sensitive adhesion in the butyl rubber is provided by mixing of the BR with a low molecular weight PIB (Vistanex). The compositions of samples examined in this work are presented in Table 1.

As is evident from the data in Figures 9 and 10, mixing elastomers (SIS and BR) with plasticizers (I for SIS and low-molecular-weight PIB for BR) and tackifying resin (R) results in an appreciable increase in retardation times (Figure 9) and corresponding reduction in relevant moduli (Figure 10). However, their effects on the values of shorter retardation time are less marked as compared with dramatic changes in the longer retardation time. It is pertinent to note that the joint effect of plasticizer and tackifying resin on the retardation

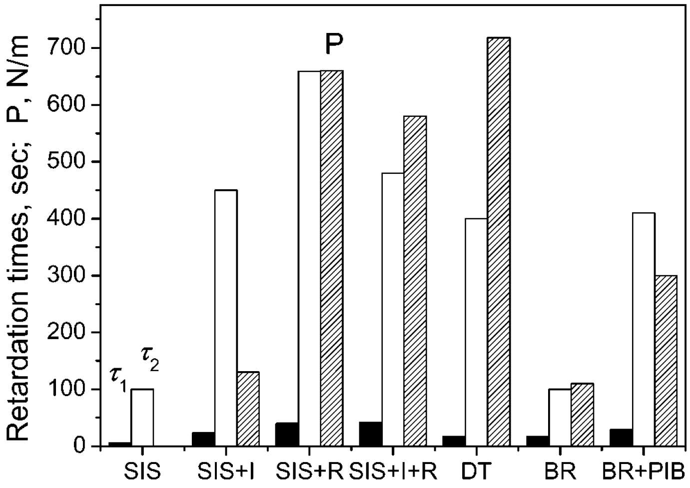

FIGURE 9 Effects of plasticizers (Isolene, I, and low-molecular-weight polyisobutylene, PIB) and tackifier resin (Regalite, R) on retardation times and peel adhesion (P) of styrene-isoprene-styrene blockcopolymer (SIS) and butyl rubber (BR) as compared with DURO-TAK 34–4230 (DT), used in this work as a typical hydrophobic PSA.

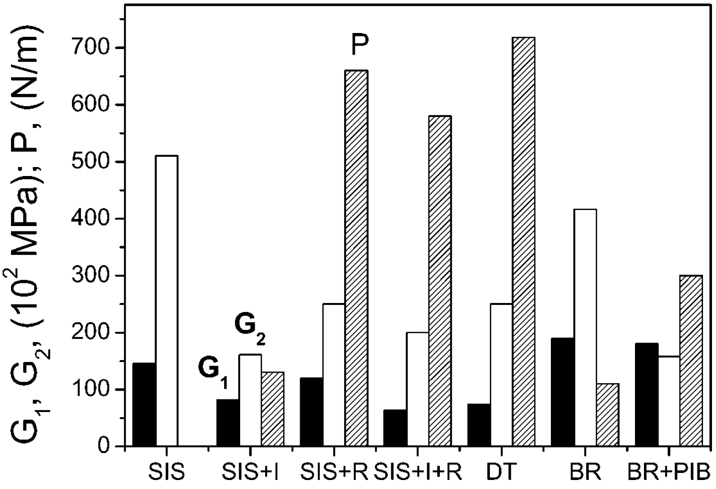

FIGURE 10 Impact of plasticizers (Isolene, I, and low-molecular-weight polyisobutylene, PIB) and tackifier resin (Regalite, R) upon the retardation moduli and peel adhesion (P) of styrene-isoprene-styrene blockcopolymer (SIS) and butyl rubber (BR) as compared with DURO-TAK 34-4230 (DT), used in this work as a typical hydrophobic PSA.

time and relevant modulus of SIS are much more pronounced than separate effects of plasticizer–tackifier mixture (compare SIS + I + R system with SIS + I and SIS + R blends in Figures 8 and 10).

Correlation between Retardation Times and Pressure-Sensitive Adhesion

The phenomena of tack, peel, and shear have been shown to depend upon the relative participation of the two primary molecular mechanisms of deformation: viscous flow that proceeds by diffusion *via* free volume, and the elastic distortion which stores free energy [8]. These two mechanisms are characterized with different timescales. Whereas the process of viscous flow requires appreciable time, the elastic one dominates at shorter timescale. To appreciate the significance of relaxation properties for adhesive behavior of polymers we have to compare the effects of composition on the relaxation and pressure-sensitive adhesion.

Figures 9 and 10 illustrate the correlation between adhesive and relaxation properties for SIS blends with the plasticizer Isolene and tackifier Regalite as well as butyl rubber plasticized with low-molecular-weight PIB. Unblended SIS and BR reveal no or low adhesion. Mixing the SIS with the plasticizer Isolene provides initial tack but comparatively low adhesion, whereas plasticizer (low-molecular-weight PIB) significantly improves both the tack and adhesion of BR. In SIS blends with the tackifier Regalite the adhesion is much improved. High adhesion is also found for triple SIS blends with tackifier R and plasticizer I. As a reference hydrophobic PSA in this work we employ a SIS-based DURO-TAK 34-4230, which demonstrates the 180-deg peel adhesion of 775 N/m. The relaxation properties of this reference sample, tested under comparable conditions, are characterized with $\tau_1 = 17\,\text{sec}$, $G_1 = 0.74\,\text{MPa}$, and $\tau_2 = 356-400\,\text{sec}$, $G_2 = 2.48\,\text{MPa}$ (Table 2, Figures 9 and 10).

Let us compare now the values found for the hydrophobic adhesives with those featured for hydrophilic PVP-PEG PSAs. The PVP-PEG system provides an appropriate model to elicit molecular structures underlying pressure-sensitive adhesion, because their adhesive behavior can be related to the changes in structure, interaction mechanism, phase state, and other physical properties as the PEG content is varied. The effects of PEG concentration on adhesive and relaxation properties of PVP-PEG blends expressed in terms of 180-deg peel force [22]; retardation times and corresponding moduli are presented in Figures 11 and 12. Whereas the shorter retardation time is nearly constant and the longer time is a monotonously

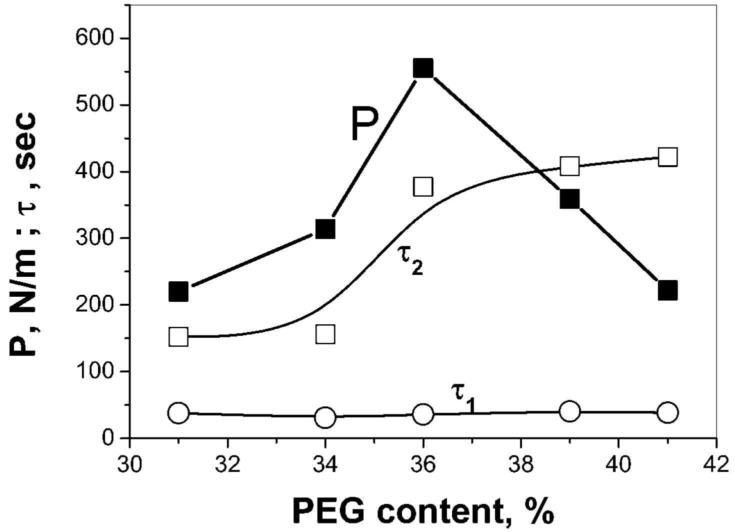

FIGURE 11 180-deg peel adhesion, *P*, and retardation times of PVP-PEG adhesives as a function of PEG concentration at 50% relative humidity of surrounding atmosphere.

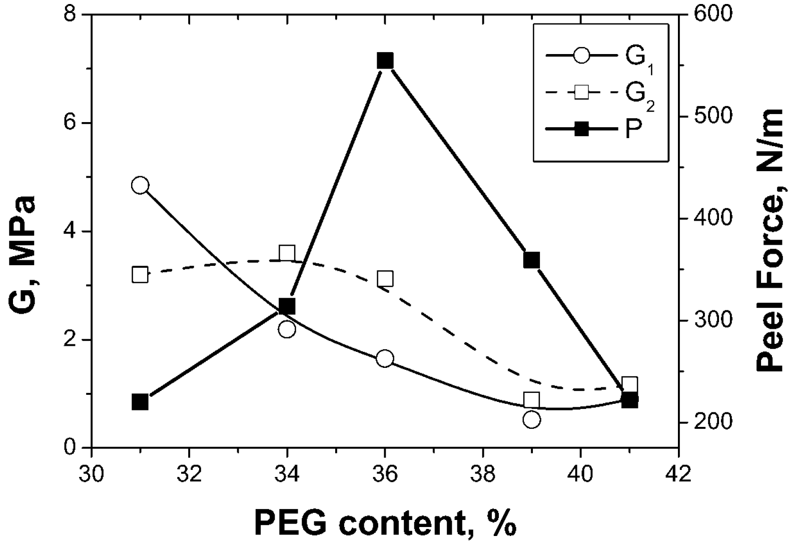

FIGURE 12 Effect of PEG concentration on 180-deg peel adhesion, *P*, and moduli corresponding to shorter (G_1) and longer (G_2) retardation times for PVP-PEG adhesives at relative humidity of 50%.

increasing function of PEG content, and relevant moduli decrease with the rise in PEG concentration between 31 and 41% PEG, the peel adhesion goes through a maximum at 36% PEG concentration in the blends. The maximum adhesion relates to the PEG concentration at which a stoichiometric PVP-PEG H-bonded complex is completely formed within the PVP-PEG blends [21]. This complex demonstrates properties that are not typical of both parent polymers. As is evident from the data in Figures 11 and 12 and Table 2, the maximum adhesion in PVP blends with 34–39% PEG is observed when the shorter and longer retardation times range within 10–65 and 120–450 sec, respectively, whereas the values of corresponding moduli vary within 0.5–2.6 and 0.8–3.8 MPa, respectively. The relaxation properties of the blend containing 36% PEG and providing best adhesion are characterized with $\tau_1 = 26-46\,\text{sec}$, $G_1 = 1.3-2.17\,\text{MPa}$, and $\tau_2 = 325-430\,\text{sec}$, $G_2 = 2.94-3.3\,\text{MPa}$.

Within the PEG concentration region (31–34%) where debonding occurs through a predominantly adhesive type of bond failure [22], the gain in adhesion is always associated with appreciable rise in the value of the longer retardation time (Figure 11). However, as PEG concentration is 36% and higher, the type of debonding is miscellaneous (adhesive–cohesive) and this rule does not hold any longer. For these blends, the longer retardation time continues to grow more smoothly, whereas the peel adhesion begins to decrease.

In the same manner as has been established above for hydrophobic blends based on SIS and butyl rubber (Figures 9 and 10), for hydrophilic adhesives the greater adhesion is associated with the values of longer retardation time ranging from 325 to 445 sec (Figures 11 and 12, Table 2). Summing up the data in Figures 9–12 and in Table 2, we come to the relaxation criteria for pressure-sensitive adhesion, which can be stated in a preliminary form as follows:

1) To be a PSA, the polymer compositions preferably possess two retardation times of 10–70 sec and 300–660 sec, respectively.
2) For proper adhesion, the relaxation modulus, G_2, relating to the longer retardation time, is preferably to be higher than the modulus, G_1, corresponding to the shorter retardation times. Because the G_2 and G_1 values are the measures of energy dissipated, respectively, for predominantly large-scale and small-scale viscoelastic mechanisms of squeeze recoil, and the amount of the energy dissipated in the course of the debonding process is the measure of adhesion, this requirement signifies the prevailing importance of

the larger-scale mechanism (that requires appreciable molecular mobility) for the pressure-sensitive adhesion.

3) Optimum adhesion is achieved as the absolute values of the G_2 and G_1 moduli ranges are in the 2.5–3.3 and 0.70–2.20 MPa, respectively.

It is evident that further work is needed to demonstrate whether the established values of retardation times and relevant moduli are also typical of the entire variety of pressure-sensitive adhesives that are currently available. Furthermore, more data should be obtained to trace quantitative correlations between the adhesion and relaxation characteristics within the window outlined by the above presented criteria. Actually, as follows from the data shown in Figures 8 and 9, the retardation times and G_1 modulus for SIS + I adhesive fall within the relaxation criteria for PSAs, yet the SIS + I adhesive exhibits relatively low peel force. This fact is most likely due to the fact that the modulus $G_2 = 1.61$ MPa for the SIS + I blend is below the lower limit outlined by the relaxation criterion ($G_2 = 2.5$ Mpa). It implies also that there exist different combinations of the retardation times and corresponding moduli, which are either favorable or unfavorable for high adhesion.

Effects of Hydrogen Bonding and Covalent Crosslinks on Relaxation and Adhesive Properties of PVP-PEG Systems

Adhesive and mechanical properties of PVP-PEG blends have been shown earlier to be controlled by the contribution of two interpenetrating networks [23, 26]. The entanglements of long PVP chains make up the first network, whereas another one is provided by hydrogen bonding through both terminal OH groups of short-chain PEG that acts as a noncovalent crosslinker of PVP chains. Accurate deconvolution of the contributions of these two networks into adhesive and mechanical properties is a difficult problem [36] and requires additional research. Adhesion tests performed with a probe method [23] showed an uncharacteristically high sensitivity to the velocity of removal of the probe, with a sharp transition from detachment by fibril formation at low probe velocity to brittle fracture at high probe velocity. This behavior implies the existence of well-defined relaxation times that govern the adhesion in hydrogen bonded PVP-PEG system.

Actually, crosslinks created by hydrogen bonding are not permanent but temporary. The intermolecular H-bonds in PVP-PEG blends can rupture and reform anew at another place during the deformation accompanying the processes of adhesive bonding and debonding. The breakup and reformation of hydrogen bonds is a time-dependent, continuous process that causes the dissipation of large energy. Indeed, based on the tan δ data the PVP-PEG adhesive has been earlier shown to be much more dissipative than classical PSAs and behaves like a liquid, whereas based on the G' data it is stiffer and provides appreciable cohesion in comparison with conventional PSAs [26].

The stoichiometric crosslinked H-bonded PVP-PEG complex, which is fully formed in the PVP blend with 36% PEG that provides the best adhesion, contains 19–20 PEG chains per 100 monomeric units of PVP [21]. High adhesion of this complex results from specific balance between large free volume because of appreciable length and flexibility of PEG crosslinks and enhanced energy of cohesion because of formation of intermolecular H-bonds. To gain an insight into the contribution of hydrogen bonds to the relaxation and adhesion of PVP-PEG adhesives, we have attempted to replace fully or partly the H-bonds in the PVP-PEG mixture with covalent bonds, leaving the same structure and large free volume in a covalent replica of the H-bonded network complex. With this purpose in mind, we have synthesized copolymers of vinyl pyrrolidone (VP) with PEG-400 diacrylate (PEGDA) and PEG-400 monomethacrylate (PEGMMA). The proposed structures of the PVP-PEG complex formed by mixing PVP and PEG-400, VP-PEGDA, and VP-PEGMMA copolymers are shown in Figure 13.

The VP-PEGDA crosslinked copolymer (Figure 13c) represents a covalent-bonded replica of a hydrogen-bonded PVP-PEG stoichiometric complex (Figure 13a). The VP-PEGDA copolymer containing about 25 PEGDA crosslinks per 100 VP units has a network density approaching the density of the H-bond network in the stoichiometric complex in the PVP-PEG mixture [21]. The major difference is that both hydrogen bonds in the PVP-PEG complex are replaced by two covalent bonds in the VP-PEGDA crosslinked copolymer. However, in the comblike copolymer VP-PEGMMA, only one of the hydrogen bonds is replaced by a covalent bond, leaving the other hydroxyl group at the end of the PEG side-chain accessible for forming a hydrogen bond with the carbonyl group in PVP (Figure 13b). The VP-PEGMMA comblike polymer (one hydrogen bond, one covalent bond) has a structure intermediate between the hydrogen-bonded PVP-PEG stoichiometric complex (two hydrogen bonds) and its covalently bonded replica VP-PEGDA copolymer (two covalent bonds). The VP-PEGMMA and VP-PEGDA copolymers spanning the entire range of monomeric compositions have been prepared.

Figure 14 compares squeeze-recoil profiles for polymer systems presented in Figure 13: PVP-PEG (36%) blend and VP-PEGDA

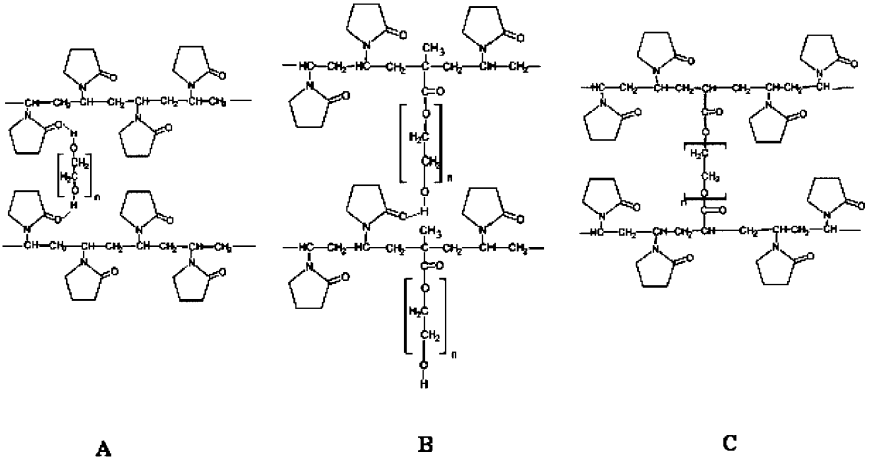

FIGURE 13 Chemical structures. (a) Stoichiometric crosslinked H-bonded complex formed in PVP-PEG blend (2 H bonds per PEG molecule, no covalent bonds between PVP and PEG). (b) The VP-PEGMMA comblike copolymer (1 H bond and 1 covalent bond). (c) The VP-PEGDA copolymer (no H bonds, 2 covalent bonds).

copolymer, which contains 25 PEGDA units per 100 VP units. Under compressive force, the sample of VP-PEGDA copolymer, which represents the covalent replica of the H-bonded PVP-PEG complex, is squeezed almost immediately until yield stress is attained and the material ceases to flow. This behavior is typical of soft gels with low modulus or viscous liquids with well-defined yield stress. However, as the sample is unloaded, it recovers its initial thickness quickly. In contrast with the PVP-PEG H-bonded network complex, the elastic recovery of covalently crosslinked material is much faster and more pronounced. This property is more featured for cured rubbers than for gels. For the latter, the contribution of nonrecoverable viscous deformation is more appreciable. The PEGMMA-VP (25:100) copolymer, wherein only a half of the H-bonds are replaced by covalent bonds, reveals intermediate behavior, but its squeeze-recoil profile overlaps with that of the H-bonded PVP-PEG (36%) adhesive. The data, therefore are not shown.

Squeeze-recoil curves in Figure 14 imply that the longer retardation time for the covalently crosslinked VP-PEGDA copolymer is expected to be lower than that typical of the H-bonded PVP-PEG complex. Indeed, as follows from the results presented in Figure 15, complete replacement of H-bonded crosslinks by covalent bonds in the

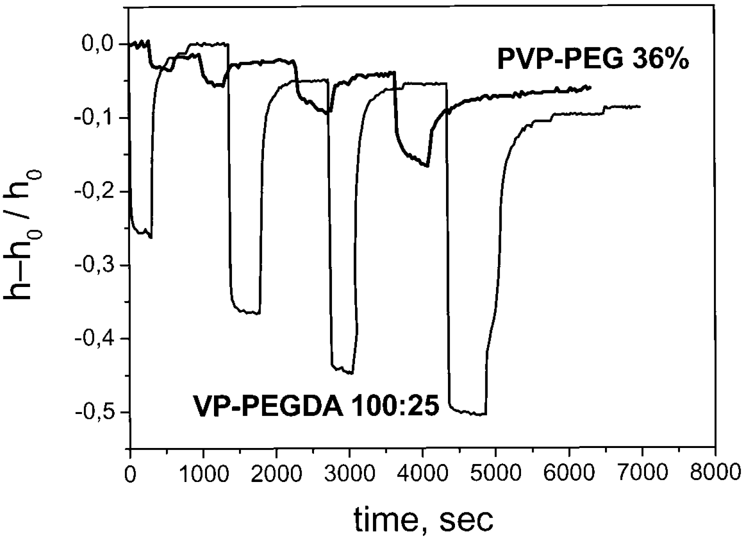

FIGURE 14 Effect of the replacement of H bonds by covalent crosslinks on squeeze-recoil profiles for PVP-PEG blends and VP-PEGDA crosslinked copolymer of comparable composition under stepwise increasing of compressive force 0.5, 1, 2, and 5 N.

VP-PEGDA crosslinked copolymer leads to dramatic drop in the longer retardation time and adhesion. If only 50% of the H bonds are replaced by the covalent crosslinks, as in the comblike VP-PEGMMA copolymer, the longer retardation time is increased compared with VP-PEGDA copolymer and, consequently, the adhesion is also improved. In this way, the results confirm unequivocally the significance of the longer retardation time and large-scale structure rearrangement component of the relaxation process for pressure-sensitive adhesion. This is in full agreement with Equation (3) which, predicts the importance of longer relaxation time and high coefficient of self-diffusion for appreciable adhesion.

The found values of retardation times and corresponding moduli for the VP-PEGDA and VP-PEGMMA copolymers are listed in Tables 3 and 4. It is instructive to compare these values with the relaxation criteria for pressure-sensitive adhesion. Nonadhesive VP-PEGDA (100:25) copolymer with 100% of covalent bonds disobeys all three of the relaxation criteria. First, the values of longer retardation time have been shown to vary from 123 to 186 sec, which is below the lower limit claimed by the first criterion (300 sec). Second, G_2 values are only insignificantly higher than G_1. Both the G_2 and G_1 values therewith

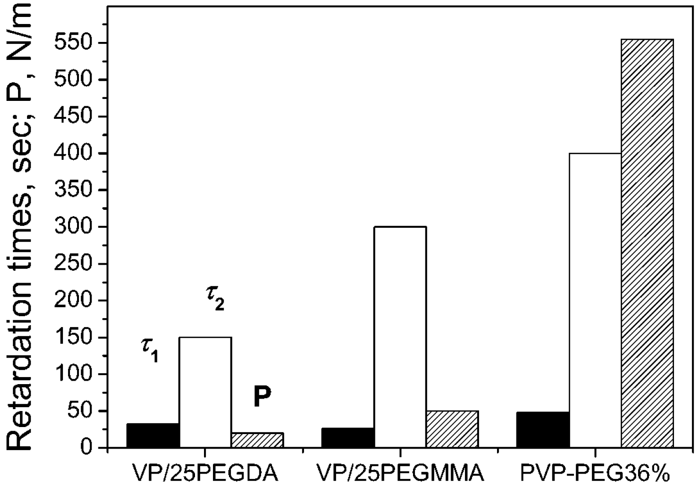

FIGURE 15 Effect of the replacement of hydrogen bonds by the covalent crosslinking of PVP macromolecules through comparatively shorter and flexible PEG-400 chains on the retardation times, τ, and peel adhesion, P. The VP-PEGDA: 0 H bonds, 2 covalent bonds per PEG chain; VP-PEGMMA: 1 H bond and 1 covalent bond; PVP-PEG: 2 H bonds and 0 covalent bonds.

depend on the compressive force, tending to increase with its reduction. And third, the absolute values of evaluated moduli ($G_2 = 0.10-0.39$ and $G_1 = 0.03-0.10\,\mathrm{MPa}$) are about one decade of

TABLE 3 Retardation Times, τ, and Characteristic Moduli, G, of Covalently Crosslinked VP-PEGDA Copolymers

Monomer composition	Compression force, N	G, MPa	τ, s	G_1, MPa	τ_1, s	G_2, MPa	τ_2, s
7.5 PEGDA/100VP	0.5	0.025	83	0.03	41	0.05	270
	1	0.033	140	0.05	51	0.05	324
	2	0.05	159	0.1	41	0.1	346
15 PEGDA/100VP	0.5	0.05	86	0.17	26	0.10	123
	1	0.10	105	0.32	13	0.12	152
	2	0.16	105	0		0	
	5	0.30	139	1.28	27	0.39	186
25 PEGDA/100VP	0.5	0.05	43	0.05	23	0.19	241
	1	0.1	46	0.1	32	0.31	152
	2	0.1	77				
PEGDA homopolymer	1	0.1	20				
	2	0.11	8				
	5	0.23	4				

TABLE 4 Retardation Times, τ, and Characteristic Moduli, G, of Comblike VP-PEGDA Copolymers

Monomer composition	Compressive force, N	G, MPa	τ, s	G_1, MPa	τ_1, s	G_2, MPa	τ_2, s
5PEGMMA/100VP	0.5	1.25	84	0		0	
	1	0.71	33	0.77	24	4.35	773
	2	1.08	109	1.45	68	3.57	384
10PEGMMA/100VP	0.2	0.33	113	0.00		0.00	
	0.5	0.53	53	1.23	10	0.88	102
	1	0.98	34	1.24	19	4.00	207
	2	0.94	77	1.73	18	1.92	209
25PEGMMA/100VP	0.2	0.30	64	0.00		0.00	
	0.5	0.53	43	0.77	26	1.50	109
	1	0.77	86	1.20	26	1.61	343
	2	1.22	75	1.69	28	3.30	445
50PEGMMA/100VP	0.5	0.63	61	0.85	38	2.00	170
	1	1.11	53	2.10	8.6	2.11	147
	2	1.54	88	2.54	26	3.25	323
	5	2.41	106	3.83	24	5.71	463
PEGMMA homopolymer	0.2	0.31	23	0.32	21	5.88	120
	0.5	0.20	79	0.40	19	0.33	218
	1	0.22	153	0.48	46	0.38	310
	2	0.29	241	0.40	134	0.77	811

magnitude lower than those stated in the third criterion for adhesion ($G_2 = 2.5{-}3.3$ and $G_1 = 0.70{-}2.20\,\text{MPa}$). Because the value of modulus is a measure of energy dissipated because of relevant process and a large dissipation of energy is needed for proper adhesion, it is no surprise that the VP-PEGDA (100:25) covalently crosslinked copolymer reveals no adhesion.

In regards to the VP-PEGMMA comblike copolymer (100:25) with 50% replacement of H bonds by covalent links, the value of the longer retardation time is at the lower border of the region stated by the first criterion for adhesion ($\tau_2 = 109{-}445\,\text{sec}$). The G_2 and G_1 moduli are approximately equal in their values ($G_2 = 2.1{-}5.7, G_1 = 2.1{-}3.8\,\text{MPa}$), and their absolute values are appreciably higher than those outlined by the third criterion for adhesion. This means that the retardation process is too hampered by insufficient compliance of material. In this way, the peel adhesion for the VP-PEGMMA copolymer is intermediate between that of 100% covalent bonded VP-PEGDA and 100% H-bonded PVP-PEG systems.

We have synthesized the VP-PEGDA and VP-PEGMMA copolymers spanning the entire range of monomer compositions. As is evident from the data presented in Tables 3 and 4, with the rise in PEGDA and PEGMMA content the longer retardation time tends to decrease and for the homopolymer of PEGDA only shorter retardation time has been found to occur. The G_2 modulus decreases with PEGMMA and tends to increase with PEGDA contents. Strictly speaking, the copolymers overloaded with PEGDA and PEGMMA should be rather regarded as crosslinked or grafted copolymers of ethylene glycol, but not as PVP crosslinked through oligomeric PEG.

In the dry state the VP copolymers with PEGDA and PEGMMA possess low or no adhesion. As is obvious from the above-presented data, the lack of adhesion is mainly because of insufficient molecular mobility of covalently crosslinked polymer embedded by the longer retardation time and relevant modulus. The impact of this mechanism can be nevertheless significantly enhanced if the VP-PEGDA or VP-PEGMMA copolymers are swollen in water, because in the swollen state both the self-diffusion coefficient of polymer segments and the retardation time are significantly increased [see Equation (3)]. And, really, the adhesion of the copolymers has been shown to increase appreciably if the amount of absorbed water is 15–40%.

Summing up the results presented in this section, we can conclude that the contribution of hydrogen bonds is of crucial importance for the development of hydrophilic pressure-sensitive adhesives. The transient character of H bonds allows their continuous breakdown and reformation in the course of material straining and relaxation, providing a tool for the dissipation of a large amount of energy during adhesive debonding or failure.

CONCLUSIONS

Under the conditions imitating the removal of compressive force upon adhesive bond formation, for which the mode of deformation is typically in shear, pressure-sensitive adhesives reveal two retardation times, which in their magnitudes are about one decade apart. The shorter retardation times (10–70 sec) define the rate of release of stored energy resulting from the recovery of conformation of polymer chains. The longer retardation times (300–660 sec) relate mainly to the energy-dissipating processes and chain entanglements, which are associated with translational movement (self-diffusion) of polymer segments and entire macromolecules in the course of larger scale structural rearrangements. Both plasticizers and tackifying resins increase the values of retardation times; however, their effects on the longer retardation time are much more pronounced as compared with the shorter time. Correlation between the adhesion and retardation time for both hydrophilic and conventional (hydrophobic) PSAs can be described fairly reasonably with Equation (3) which, relates peel adhesion to the relaxation time and translational mobility of adhesive polymer. For the hydrophilic PVP-PEG PSAs, the contribution of intermolecular hydrogen bonding is of crucial importance to their adhesive and relaxation behaviors.

REFERENCES

[1] Tschoegl, N. W., *Mechan. Time-Depend. Materials* **1**, 3–31 (1997).

[2] Satas, D. *Handbook of Pressure-Sensitive Adhesive Technology*, (Ed.) (Satas & Associates, Warwick, RI, 1999), 3rd ed.

[3] Dillard, D. A. and Pocius, A. V. *The Mechanics of Adhesion*, (Eds.) (Elsevier Science, New York, 2002).

[4] Zosel, A., *J. Adhes. Sci. Technol.* **11**, 1447–1457 (1997).

[5] Tschoegl, N. W., *The Phenomenological Theory of Linear Elastic Behavior* (Springer-Verlag, Heidelberg, Germany, 1989), p. 126.

[6] Ferry J. D., *Viscoelastic Properties of Polymers*. (Wiley and Sons, New York, 1980) 3rd Ed.

[7] Schramm, G., *A Practical Approach to Rheology and Rheometry* (Haake Rheometers, Karlsruhe, 1994), p. 104.

[8] Rohn, C., Rheology of Pressure Sensitive Adhesives, in *Handbook of Pressure-Sensitive Adhesive Technology*, D. Satas (Ed.) (Satas & Associates, Warwick, RI, 1999), 3rd ed., pp. 153–170.

[9] Kaelble, D. V., Theory and Analysis of Peel Adhesion, in *Handbook of Pressure-Sensitive Adhesive Technology*, D. Satas (Ed.) (Satas & Associates, Warwick, RI, 1999), 3rd ed., pp. 104–120.

[10] Feldstein, M. M., Chalykh, A. E., Chalykh, A. A., Fleischer, G., and Siegel, R. A., *ACS Polym. Mater. Sci. Eng.* **81**, 467–468 (1999).

[11] Feldstein, M. M., Chalykh, A. E., Vartapetian, R. Sh., Kotomin, S. V., Bairamov, D. F., Borodulina, T. A., and Geschke, D., *Proceed. 23rd Annual Meeting Adhesion Soc.* 55–57 (2000).

[12] De Gennes, P. G., *J. Chem. Phys.* **55**, 572–580 (1971).

[13] Feldstein, M. M., Chalykh, A. E., and Platé, N. A., *Proceed. 5th European Conference on Adhesion (EURADH 2000)*, Lyon, 176–181 (2000).

[14] Feldstein, M. M., Chalykh, A. E., Chalykh, A. A., and Platé, N. A., *ACS Polym Mater. Sci. Eng.* **81**, 465–466 (1999).

[15] Feldstein, M. M., Platé, N. A., Chalykh, A. E., and Cleary, G. W., PCT Application WO 02/04570 (2002); U.S. Patent 6, 576, 712 (2003).

[16] Feldstein, M. M., Platé, N. A., Chalykh, A. E., and Cleary, G. W., *Proceed. 25th Annual Meeting Adhesion Soc. & 2nd World Congress Adhesion Relat. Phenom.* **1**, 292–294 (2002).

[17] Cleary, G. W., Feldstein, M. M., Singh, P., and Platé N. A., *Proceed. Intern. Symp. Control. Release Bioactive Mater.* **30**, 123 (2003).

[18] Feldstein, M. M., Lebedeva, T. L., Shandryuk, G. A., Kotomin, S. V., Kuptsov, S. A., Igonin, V. E., Grokhovskaya, T. E., and Kulichikhin, V. G., *Polym. Sci.* **41**(8), 854–866 (1999).

[19] Feldstein, M. M., Lebedeva, T. L., Shandryuk, G. A., Igonin, V. E., Avdeev, N. N., and Kulichikhin, V. G., *Polym. Sci.* **41**(8), 867–875 (1999).

[20] Feldstein, M. M., Kuptsov, S. A., Shandryuk, G. A., and Platé, N. A., *Polymer* **42**(3), 981–990 (2001).

[21] Feldstein, M. M., Roos, A., Chevallier, C., Creton, C., and Dormidontova, E. D., *Polymer* **44**(6), 1819–1834 (2003).

[22] Chalykh, A. A., Chalykh, A. E., Novikov, M. B., and Feldstein, M. M., *J. Adhes.* **78**(8), 667–694 (2002).

[23] Roos, A., Creton, C., Novikov, M. B., and Feldstein, M. M., *J. Polym. Sci., Polym. Phys.* **40**, 2395–2409 (2002).

[24] Bairamov, D. F., Chalykh, A. E., Feldstein, M. M., Siegel, R. A., and Platé, N. A., *J. Appl. Polym. Sci.* **85**, 1128–1136 (2002).

[25] Bairamov, D. F., Chalykh, A. E., Feldstein, M. M., and Siegel, R. A., *Macromol. Chem. Phys.* **203**(18), 2674–2685 (2002).

[26] Novikov, M. B., Roos, A., Creton C., and Feldstein, M. M. *Polymer* **44**(12), 3559–3576 (2003).

[27] Li, Y., Zhang, R., Chen, H., Zhang, J., Suzuki, R., Ohdaira, T., Feldstein, M. M., and Jean, Y. C., *Biomacromolecules*, **4**, 1856–1864 (2003).

[28] Vartapetian, R. Sh., Khozina, E. V., Kärger, J., Geschke, D., Rittig, F., Feldstein, M. M., and Chalykh, A. E., *Colloid Polym. Sci.* **279**(6), 532–538 (2001).

[29] Vartapetian, R. Sh., Khozina, E. V., Karger, J., Geschke, D., Rittig, F., Feldstein, M. M., and Chalykh, A. E., *Macromol. Chem. Phys.* **202**(12), 2648–2652 (2001).

[30] Dahlquist, C. A., in *Treatise on Adhesion and Adhesives*, Patrick R.L. (Ed.) (M. Dekker, New York, 1969), Vol. 2, pp. 219–260.

[31] Kotomin, S. V. and Kulichikhin, V. G., *Polym. Sci.* **38**, 498–502 (1996).

[32] Kotomin, S. V., Borodulina, T. A., Feldstein, M. M., and Kulichikhin, V. G., *Proceed. XIIIth Intern. Congress on Rheology*, Cambridge, UK, **4**, 44–46 (2000).

[33] Laun, H. M., *Macromol. Chem., Macromol. Symp.* **56**, 55–66 (1992).

[34] Meeten, G. H., *Rheol. Acta* **41**, 557–566 (2002).

[35] Ward, I. M., *Mechanical Properties of Solid Polymers*, Wiley, New York, 1983, Chap. 5.

[36] Creton, C., Roos, A., Novikov, M. B., and Feldstein, M. M., *Proceed. 26th Ann. Meeting Adhes. Soc.* 34–36 (2003).